Stability of the LEO Environment as a Dynamical System

Daniel Jang[*], **Andrea D'Ambrosio**[†], **Miles Lifson**[‡], **Celina Pasiecznik**[§], **Richard Linares**[¶]
Massachusetts Institute of Technology

ABSTRACT

The new space age has brought with it a congested Low Earth Orbit (LEO) environment, where new commercial and government large LEO constellations (LLC) are being proposed at a faster rate that require strict management of the orbital architecture. Effective policies and technologies to enable deorbiting measures for post mission disposal (PMD) and active debris removal (ADR) are needed to remove payloads that are past their lifetimes and other debris objects. Anthropogenic fragmentation events such as destructive anti-satellite tests produce thousands of debris pieces. Natural conjunctions happen as well, with around 300 on-orbit fragmentation events having occurred to date. As the number of satellites and debris continue to grow, it is imperative to calculate the relative and absolute risk of collisions in LEO.

There are largely two methods to model the evolution of the LEO ASO population and collision risk: statistical sampling methods such as Monte Carlo methods, and source-sink models, also known as particle-in-box models. Statistical sampling methods propagate every ASO's orbital states with high fidelity propagators to estimate the future space environment at some small timesteps. Computing a debris environment with different sets of assumptions, however, requires high computational cost as each object must be propagated. Source-sink models describe the interactions between populations of objects with ordinary differential equations. Average values are often used to set the parameters of each species of population. This method removes the need for computationally expensive propagation of every ASO states to estimate the future debris environment. MIT Orbital Capacity Tool (MOCAT) has recently been developed, which is an evolutionary dynamical system model to analyze the evolution of the LEO ASO population. The LEO environment is modeled as a multi-shelled system with a feedback control loop, where some parameters such as launch rate and PMD rate can be set as the control variable for some cost optimization.

In this paper the effect of expanding the populations to multiple species to span a wider set of parameters is explored. For example, from the 3-species MOCAT model consisting of payload, derelict, debris species, the debris population is divided into large and small debris populations to create a 4-species model, whose dynamics is then analyzed. The additional sampling of the species result in a different population evolution compared to the original generalized property, as the interaction with the other species and atmospheric deceleration affect the expanded species differently. Separately, a 5-species model is created by expanding the 3-population model with the payload and derelict objects each expanded into large and small populations. These models are evaluated for scenarios initialized with the MASTER 8 debris population for 2020, atmosphere modeled with the average solar cycle in JB2008 and future launch profile from International Telecommunication Union (ITU) filings as well as multiples of the filings as the replacement-level launch rate to replenish the future constellations. A Monte-Carlo method is also being developed to validate the source-sink model. This method is used to estimate the collision probability for the source-sink model using the Cube method. Preliminary results from this development is also described in this paper. The results from this analysis shows that using singular average values for the ASO species' physical characteristics may be too simplified — additional sampling of the varied population to model them as separate populations result in a higher fidelity modeling and can yield different outcomes.

[*]Ph.D. Candidate, Department of Aeronautics and Astronautics, E-mail: djang@mit.edu
[†]Postdoctoral Associate, Department of Aeronautics and Astronautics. E-mail: andreada@mit.edu
[‡]Ph.D. Candidate, Department of Aeronautics and Astronautics. E-mail: mlifson@mit.edu
[§]SM Candidate, Department of Aeronautics and Astronautics. E-mail: cpasiecz@mit.edu
[¶]Rockwell International Career Development Professor, Associate Professor of Aeronautics and Astronautics, Department of Aeronautics and Astronautics. E-mail: linaresr@mit.edu

1. INTRODUCTION

Cheaper and more reliable launches into Low Earth Orbit (LEO) in the past decade have led to a new space age. Until recently the increase in object number in space was around 300 objects per year; however, increased launch cadence and the rise of large LEO constellations (LLC) has led to a marked increase in LEO population. The US Federal Communications Commission (FCC) and the United Nation's International Telecommunication Union (ITU) filings show that companies or governments are getting approvals for constellations that are greater than the current number of objects in space. For example, in 2021 the government of Rwanda has filed with the ITU a constellation of 327,230 satellites, and a Canadian company Aether has filed for a constellation with 115,000 satellites [1, 2]. Though it's not a certainty that these constellations will all be launched, the increase in commercial interest for LLC has made commercial and governmental stakeholders concerned about the sustainability of the LEO environment.

1.1 Modeling the LEO environment

Over the years, studies have shown the dangers of this increased population, and policies and metrics have been proposed to counter the increased risk in the space environment. Computing the LEO orbital capacity requires an understanding of the risk of collisions and the stability of the LEO environment. Ever-increasing launch-rate due to proposed megaconstellations pose an unprecedented increase in risk for conjunction, as collision probability grows as N^2. Kessler's seminal paper in 1971 originally described the potential for runaway growth of orbital debris due to debris causing more debris through collisions, which could lead to an unusable orbital environment [3]. Since then, several analytical methods have been proposed in literature to better quantify this risk.

There are largely two methods to model the evolution of the LEO ASO population and collision risk: statistical sampling methods such as Monte Carlo methods, and source-sink models, also known as particle-in-box models. Statistical sampling methods propagate every ASO's orbital states with high fidelity propagators to estimate the future space environment at some small timesteps. This method allows for accurate near-future predictions of potential collisions and is used operationally today for conjunction avoidance. Existing models include NASA's Orbital Debris Engineering Model (ORDEM) and LEGEND, European Space Agency's Orbital Debris Evolutionary Model (ODEM), Chinese Academy of Sciences' SOLEM (Space Objects Long-term Evolution Model), University of Southampton's Debris Analysis and Monitoring Architecture for the Geosynchronous Environment (DAMAGE) and more. For each of these models, the debris population and densities are outputted for some initial condition and assumptions. Computing a debris environment with different sets of assumptions, however, requires high computational cost as each object must be propagated. Sampling over a distribution of uncertainties on the states and parameters would require an exponential number of propagations. The high cost is due to the small time steps required to accurately model a collision and semi-analytical propagators requiring high compute cost to propagate far into the future. For each collision or fragmentation event, some breakup model such as NASA Standard Breakup Model is used to model the debris cloud generation. Though the outputted debris distribution for some assumed initial condition and future traffic model exist, all of these models are closed-source and inputting arbitrary assumptions is difficult if not impossible.

Evolutionary models describe the interactions between populations of objects with ordinary differential equations. For example, if all space objects of interest are categorized as payloads, derelict satellites or debris, three ordinary differential equations can describe the interaction between these populations, much like the Lotka–Volterra systems of equations also known as predator-prey and source-sink models. Average values are often used to describe the population's characteristics, such as a population's size, velocity, rate of launch and failure-rate. This simplification removes the need for computationally expensive propagation of individual object states to estimate a future debris environment. Gross populations are propagated forward according to the governing differential equations, which allows for fast solutions even far into the future. Exploration of a wide set of initial conditions and parameters is much more approachable. Kessler and Cour-Palais first described the feedback runaway phenomena and identified the risk of an exponential increase in the number of space debris, and since then a few evolutionary models have been proposed in the literature. Talent introduces the particles-in-box (PIB) model where a population within an orbital shell is assumed to have some average characteristic and interactions. Fast Debris Evolution (FADE) used simplified first order differential equations to describe the population interaction. JASON describes a three-population model for one shell and a given launch cadence [4]. While other models have expanded the evolutionary model to analyze multiple shells, optimal control schemes and economic equilibrium for maximum policy intake, none have analyzed the multi-shell stability using evolutionary models, inclusion of non-circular orbits and periodic atmospheric density fluctuations. A higher fidelity evolutionary model will require these attributes, and that is described in this work.

There are many unique aspects to the MIT Orbital Capacity Assessment Tool (MOCAT). The tool uses the PIB formulation shown in the literature, where the interactions between species is defined by ordinary differential equations. It is flexible in defining a number of populations to model. The base set of ordinary differential equations used in the 3-species model — typically as payload (S), derelict satellites (D) and lethal debris (N) — has been modified from the model in [5], and is described in Eq. 1.

MOCAT is being developed to assess the stability of the LEO environment in a generalized manner. Its use of a few types of species means only a limited number of ways exist to differentiate the species, typically using averaged values. A few indexes have been proposed in the literature to calculate the environmental criticality of each ASO object in LEO [6–8], and it has been shown that the size, mass and altitude of the object contribute heavily to its potential to be part of a catastrophic fragmentation event. The use of generalized values for physical parameters in each species in the SSEM model may not capture the full spectrum of existing ASOs, which can then misrepresent the timescale at which the debris population dynamics change. An object's fragmentation potential has a non-linear relationship to its physical properties such as mass and size as shown in Eqs. **??** and in Fig. 3. Due to this, the degree to which ASOs experience atmospheric drag is also affected nonlinearly. This paper addresses this gap by proposing a method to divide the mass of the object for a given species and analyzing the effect of a higher resolution sampling of the physical property of each species.

In order to validate this model, a more traditional method of simulating the LEO environment can be used using Monte-Carlo methods. A number of models have been developed by space agencies and private groups, such as LEO to GEO Debris model (LEGEND) has been developed by NASA [9], DAMAGE model from United Kingdom Space Agency [10, 11], MEDEE model from Centre National d'Etudes Spatiales [12], DELTA model from European Space Agency [13], LUCA model from Technische University at Braunschweig [14],and NEODEEM model from Kyushu University and the Japan Aerospace Exploration Agency, FAST [4], IMPACT [15], and others [16–18]. Though much of the models are proprietary, an Inter-Agency Space Debris Coordination Committee (IADC) study in 2013 compared many of the models in [19]. As noted, most of these models use the same assumptions, breakup models, etc which may contribute to bias on the results, but it is also seen that even for very simple scenarios such as "no new launches" or "business as usual (BAU)" the models can vary in its outputs. The randomized initial sampling of the initial distribution of ASOs used by these MC methods prove to be important as seen by the fact that for all of the models, the results span a wide range.

This paper is organized as follows:

- Section 1 introduces the problem, literature review and motivation for this work, along with the base MOCAT model architecture.
- Section 2 describes the 4- and 5-species MOCAT models used for the analysis of expanded population parameter modeling.
- Section 3 shows the results from the numerical simulations.
- Section 4 summarizes the conclusions of the work.

2. MIT ORBITAL CAPACITY ASSESSMENT TOOL (MOCAT) MODEL

The MIT Orbital Capacity Assessment Tool (MOCAT) is a family of multi-bin multi-species source-sink models to study the evolution of the LEO environment, with different versions modeling different species and cross-species interactions [20–24]. MOCAT-3 models the LEO environment using three populations: payloads, derelicts, and debris. MOCAT-3 has been used to estimate LEO orbital capacity using stability criteria to maximize launch rate while keeping the environment stable and for varying degrees of payload failure rates [20, 25]. MOCAT-4S models the use of concentric specially phased orbital shells of "slots" for large constellations that inherently avoid collisions and was used to demonstrate a method to estimate benefits to space sustainability and spaceflight safety from slotting [22, 23]. MOCAT-4N subdivides debris into trackable and lethal untracked debris population and includes a radar model to model debris custody and detectability [21].

Similar to other SSEM models, MOCAT generalizes population parameters such as mass and diameter to some average value. For example, previous MOCAT iterations modeled payload and derelict populations as featuring an average size

of 1.49 m and average mass of 223 kg as chosen in [26]. In this paper, we introduce new functionalities and parameters, and compare their contribution to the orbital capacity by analyzing a 4-population model with an additional debris species with a property, and a 5-population model with expanded payload and derelict populations each with different properties from the original species. This work will show how the discretization of parameters for each species can allow for modeling a range of parameters for a population species, especially for parameters that exhibit non-linear effects on the population derivatives.

A brief description and assumptions of the general MOCAT model and the main interactions are presented below. The full set of assumptions and methodologies can be found in the relevant work above.

The key model parameters and assumptions are shown here to summarize the MOCAT model. First, a 4-species MOCAT model will be described. While MOCAT-4S included two debris populations (tracked and untracked) the physical characteristics and therefore the interaction with other populations and with the space environment was identical. The 4-species model used in this paper will also have two types of debris populations; however, both debris types will differ in physical characteristics.

In this model, the LEO ASOs will be divided into payload (S), derelict satellites (D), and debris (N). Slotted spacecraft indicate on-station spacecraft station-keeping to maintain position within slots within near-circular compatible shells, whereas unslotted spacecraft indicates satellites not designed to feature compatible orbits. Derelict satellites represent intact satellites that fail to meet the post-mission disposal guidelines and remain on-orbit, but without the ability to perform collision avoidance maneuvers.

The dynamics for the MOCAT model is described by a system of ordinary differential equations as such:

$$\dot{\boldsymbol{P}} = \dot{\boldsymbol{\Lambda}} + \dot{\boldsymbol{C}}_{PMD} + \dot{\boldsymbol{F}} + \dot{\boldsymbol{C}} \tag{1}$$

where each term is meant to be function of time and altitude shell. For example, the three species model with payload (S), derelict (D), and debris (N) populations, the population vector can be described as $\boldsymbol{P}(h,t) = [S(h,t), D(h,t), N(h,t)]$ where h is the shell number and t describes the time index. For a model with greater number of species, additional elements are appended to $\boldsymbol{P}(h,t)$.

$\dot{\boldsymbol{\Lambda}}$ is the launch rate in objects per year. For a scenario where only the payload class has launches, $\dot{\boldsymbol{\Lambda}} = [\lambda_s, 0, 0, ...]$ where λ_s is the yearly launch rate for the payload species.

$\dot{\boldsymbol{C}}_{PMD}$ describes the effect of post-mission disposal, which is the controlled process of removing an active satellite after its useful lifetime has ended. Most LEO satellites with enough propellant will have such a plan to remove itself from the space environment safely. A failed PMD will contribute to the space debris problem, and the model will then categorize the payload S as a derelict object D, and the rate at which this occurs is described by $\dot{\boldsymbol{C}}_{PMD}$. The PMD success rate is described by P_M and the operational lifetime of the payload population is Δt years.

$\dot{\boldsymbol{F}}$ describes the population changes within a shell due to atmospheric drag and the consequent altitude decay. Active satellites are assumed not to be subject to the decay effects since they can perform station-keeping maneuvers to remain in their orbit. Therefore, only derelicts and debris experience the orbital decay effects.

$$\dot{\boldsymbol{F}} = \left[0, \dot{F}_{d,D}, \dot{F}_{d,N}, 0\right] \tag{2}$$

Indicating with Q the number of objects belonging to a generic species, $\dot{F}_{d,Q}$ can be written as follows:

$$\dot{F}_{d,Q} = -\frac{Q_+ v_+}{d} + \frac{Qv}{d} \tag{3}$$

where d is the thickness of the shell, and the subscript + refers to the quantities related to the shell right above the current one. v is the rate of change of the semi-major axis, expressed as:

$$v = -\rho B \sqrt{\mu R} \tag{4}$$

In Eq. (4), μ is the Earth gravitational parameter; R is the radial distance of the objects with respect to the center of the Earth (the assumption of near-circular orbits is here carried out, such that the semi-major axis corresponds to the radial distance); $B = c_D \frac{A}{m}$ is related to the ballistic coefficient with $c_D = 2.2$ [27]. A is the area of the object, and m is the mass of the object. ρ is the atmospheric density, computed as a static exponential model from CIRA-72 [28].

$$\rho = \rho_0 \exp\left(-\frac{h-h_0}{H}\right) \tag{5}$$

where h is the altitude of the object, ρ_0 is the atmospheric density at reference altitude h_0, and H is the atmospheric scale height [29]. $\dot{\boldsymbol{C}}$ describes the population change due to collision dynamics between the species as

$$\dot{\boldsymbol{C}} = [\dot{C}_S, \dot{C}_D, \dot{C}_N, ...]. \tag{6}$$

The number of fragments generated by each type of collisions n is derived from the NASA standard break-up model [30], where the collisions are categorized as catastrophic and non-catastrophic depending on the released energy of the impact. The number of fragments caused by a catastrophic and non-catastrophic collisions are denoted as n_c and (n_{nc} respectively. In MOCAT, collisions are considered catastrophic between intact objects (e.g. S, D) and non-catastrophic for collisions involving debris.

$$n_c = 0.1\, L_C^{-1.71} (M_i + M_j)^{0.75} \tag{7}$$

$$n_{nc} = 0.1\, L_C^{-1.71} (M_p \cdot v_{imp}^2)^{0.75} \tag{8}$$

where M_i, M_j are the mass of object i and j respectively, M_p is the mass of the lighter object, L_C is the characteristic length, and v_{imp} is the impact velocity assumed to be for all collisions 10 km/s, which is accurate for the vast majority of collisions between two random LEO objects [26].

To organize the collision interactions and input parameters, a particular species' population changes due to collisions can be described with:

$$\dot{C}_i = \sum_{j=1}^{N_s} \Gamma_{ij} \phi_{ij} Q_i Q_j + \dot{C}_{i,add} \tag{9}$$

where N_s is the number of species considered (in this work $N_s = 4$), $i, j = 1, ..., N_s$ are the subscripts indicating each generic species Q, and Γ_{ij} stores the various coefficients. A detailed description is found in [20–22] and is expanded in the following section.

Size-dependent probability of collision between two objects is defined as

$$\phi_{ij} = \pi \frac{v_r(h)(r_i + r_j)^2}{V(h)} \tag{10}$$

where $v_r(h)$ represents the relative impact velocity, in this work assumed to be constant and equal to 10 km/s, $V(h)$ is the volume of the orbital shell, and $r_{i,j}$ is the radius of the object.

3. MOCAT-MC MODEL

A Monte-Carlo approach has been implemented for MOCAT called MOCAT-MC, which is a full-scale three-dimensional debris evolutionary model to assess the LEO ASO population. MOCAT-MC propagates individual objects and models the interaction between objects at each time step. As described earlier, this method is computationally expensive, though is able to model and track individual objects' orbital and interaction history. Individual objects' parameters and trajectories at each time-step are adjustable, allowing for specific orbital maneuvers or change of physical parameters for specific satellites.

The flowchart schematic for the MOCAT-MC tool is shown in Fig. 1. As a Monte-Carlo tool, a simulation consist of many episodes is run with some sampling of one or more random variables with associated given probability distribution functions (PDF). The random variables to be sampled and the PDFs can vary depending on the analysis to be performed. A number of inputs are given for the simulation. The propagator, scenario duration and the propagation time step will be chosen. The SGP4 propagator by US Space Force (USSF) is currently implemented, while other semi-analytical and analytical propagators will also be available in the future to allow for a range of modeled perturbations, fidelity and computational speed. The initial ephemeris is also loaded, which can be seeded with an existing catalog

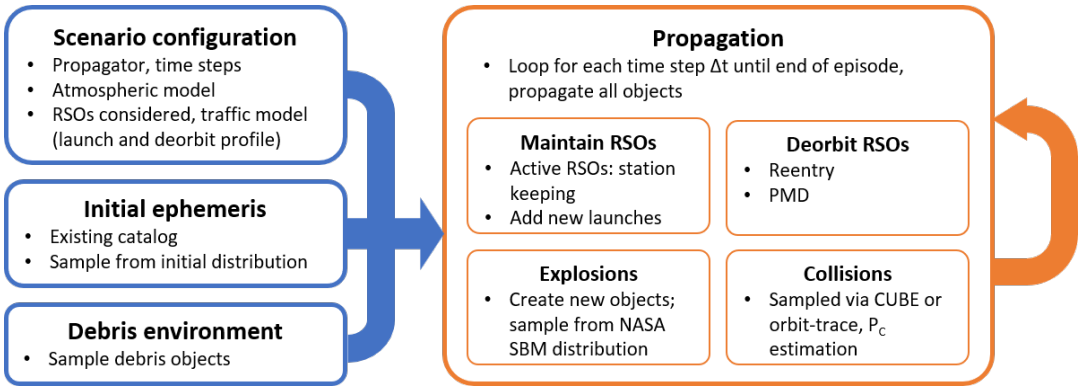

Fig. 1: Schematic for the Monte Carlo tool MOCAT-MC

such as the Two Line Element (TLE) catalog provided publicly by the 18th Space Defense Squadron. Alternatively, a range orbital parameters can be provided which can be sampled to seed the initial orbital distribution. Each object can have a unique lifetime, station-keeping methods, failure rate, size, etc to characterize its behavior and potential interaction with other objects. Lastly, the initial debris environment can be initialized. Depending on the analysis, the size, number and orbital parameters of these objects can be set. The minimum size debris to be considered in the model will also be an input parameter, which will affect the number of objects in the simulation. The PDF of the debris population parameters can be supplied from LEO debris models such as ESA's MASTER model [31].

After the initialization step, MOCAT-MC will enter the propagation loop. For each propagation step, the satellite states are propagated by the chosen time step Δt and the following calculations are executed:

- Active RSOs are maintained, such that existing satellites maintain their orbital altitude to counteract the atmospheric drag. New launches adds RSOs to the simulation, either with a deterministic launch date and orbital profile or sampled from some PDF of launch rate and final orbits.
- Some RSOs are deorbited and removed from the simulation. Objects with low apogees are removed due to atmospheric reentry. Active satellites at the end of the lifetime are removed due to PMD; however, some of these satellites will fail to PMD with some given probability, which will change its status to an inactive or derelict satellite. These satellites will unable to maintain their orbital altitude and decay due to atmospheric drag.
- RSOs will explode with some given probability, usually intact objects such as payloads, derelict objects and rocket bodies. An explosion will spawn new smaller objects, and the quantity, direction and size of the new objects will be sampled from the NASA Standard Breakup Model EVOLVE 4 for low-intensity and high-intensity explosions [30].
- Similar to explosions, collisions will produce new objects in the simulation. The parameters of the new objects resulting from the collision will follow EVOLVE 4, and are described in Eqs. 8 and 7. To determine collision between two objects, the CUBE method is used [32, 33].

4. EXPANDING THE SPECIES PARAMETERS

The inherent architecture of SSEM models necessitates the use of one value associated with each parameter of a population, typically an average. For example, all payloads and derelict objects in the previous MOCAT models were generalized to objects with mass $m = 223$ kg and cross sectional area $A = 1.741$ m^2 [20–23]. The generalized approach of SSEM models allows for faster computation, though with lower fidelity, and the number of species is limited to capture the evolution of the population dynamics with limited computational cost. In reality, the objects in space vary wildly in size and shape, and the effect of generalizing these into singular average values has not been studied. Debris objects in particular can range multiple orders of magnitude in size and number [15]. To address this gap, population parameters can be discretized and sampled at a higher rate rather than using one average value. One such parameter

that has been discretized for all MOCAT models and most other SSEM models has been the altitude parameter, which is usually discretized into equi-spaced shells. This limits interaction between species to intra-shell populations which is more realistic, and it more closely models the vastly different role the atmospheric sink plays at each altitude. A finer discretization scale may seem to allow for higher fidelity simulations, though it has been shown that after 30 or so LEO altitude bins, the fidelity gain is limited [26].

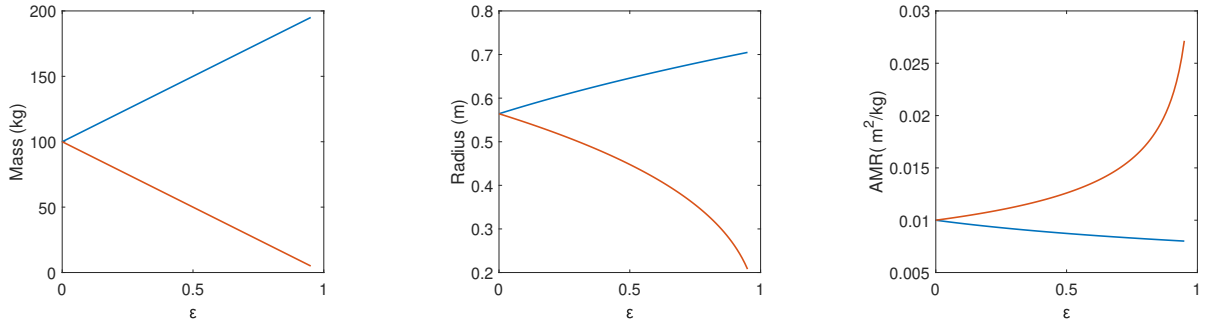

(a) Mass vs ϵ (b) Radius vs ϵ (c) AMR vs ϵ

Fig. 2: Notional physical attribute scaling for ϵ for constant mean mass and density

Fig. 3 shows the effect of different area-to-mass ratio (AMR) has on deorbit duration for low to high solar activity periods. Iso-density analysis is done to keep the density of a species the same, which leads to a varied AMR for varied size of the object.

4.1 Expanded debris population for a 4-species model

As described in Section 2 the collision interaction between species contributes to the overall population via $\dot{\boldsymbol{C}}$ in Eq. 1. The pairwise interactive term for the expanded 4-species model is broken down into each interactive element in Table 1. The debris population is divided into an additional population with a different physical characteristic - in this case, the mass of the object is additionally sampled.

A new parameter ϵ is introduced to divide the population into two populations. In this model we divide the mass of the original debris population into two species of differing mean masses, though the ensemble debris population's mass is fixed at $\bar{m}_{N0} = 0.64$ kg. For a given $\bar{m}_{N0}$, the ϵ parameter will allow for the mean of the two new species to grow apart until the smaller debris mass $m_M = 0$ and the larger debris mean mass $m_N = 2\bar{m}_{N0}$. There are non-linear implications of keeping constant the ensemble debris population mean mass, as $m \sim b^{1/3} \sim A^{2/3}$. While keeping the mean mass equivalent to a model with fewer species, the subdivided population will experience different population dynamics such as collision probability, atmospheric drag effects, collision fragmentation dynamics, etc. Rather than

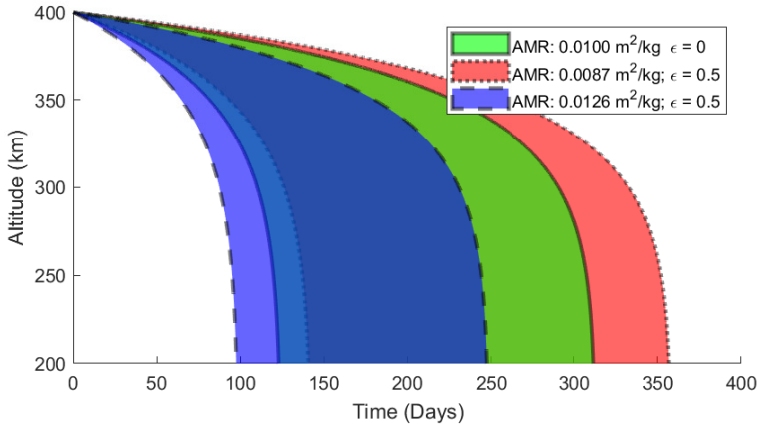

Fig. 3: AMR vs decay of satellites from 400 kim circular altitude for F10.7 index between 70 to 200 sfu

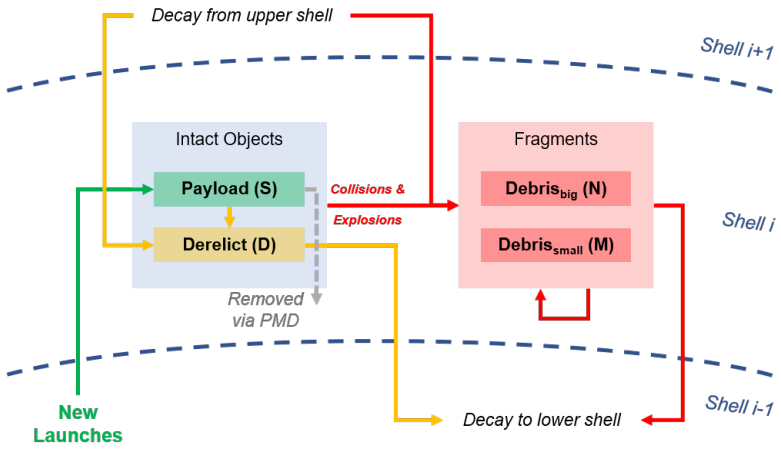

Fig. 4: Schematic for the 4-population model that includes an expanded debris population.

describing the entire debris population with one mass, this will allow a finer sampling, and its implications explored. The fragmentation dynamics is described in Eq. 8, where the number of the non-catastrophic fragments $n_{nc} \sim M^{0.75}$.

Table 1: Pairwise interactions between the species for the expanded debris model (4-species model)

	Species	**S (Slotted satellites)**	**D (Derelicts)**	**N (Larger Debris)**	**M (Smaller Debris)**
$\dot{\mathbf{C}}$ **Collision Source**	**S**	$-\alpha_a \phi_{11} S^2$	$\delta S(\phi_{12} D + \phi_{13} N + \phi_{14} M)$	$n_{11}\phi_{11}\alpha_a S^2 + n_{12}\phi_{12}\alpha SD + n_{13}\phi_{13}\alpha SN + n_{14}\phi_{14}\alpha SM$	$n_{11}\phi_{11}\alpha_a S^2 + n_{12}\phi_{12}\alpha SD + n_{13}\phi_{13}\alpha SN + n_{14}\phi_{14}\alpha SM$
	D	$-\phi_{12}(\delta+\alpha)SD$	$-\phi_{22} D^2$	$n_{22}\phi_{22} D^2 + n_{23}\phi_{23} DN$	$n_{22}\phi_{22} D^2 + n_{23}\phi_{24} DM$
	N	$-\phi_{13}(\delta+\alpha)SN$	$-\phi_{23} ND$	$n_{33}\phi_{33} N^2$	$n_{34}\phi_{34} NM$
	M	$-\phi_{13}(\delta+\alpha)SM$	$-\phi_{24} MD$	$n_{34}\phi_{34} NM$	$n_{44}\phi_{44} M^2$
m Mass [kg]	-	223	223	$(1+\varepsilon)\bar{m}_{N0}$	$(1-\varepsilon)\bar{m}_{N0}$
b Diameter [m]	-	1.5	1.5	$(1+\varepsilon)^{1/3} b_{N0}$	$(1-\varepsilon)^{1/3} b_{N0}$
A Area [m^2]	-	1.77	1.77	$(1+\varepsilon)^{2/3} A_{N0}$	$(1-\varepsilon)^{2/3} A_{N0}$

Table 2: Simulation input parameters

h_{min}	h_{max}	N_{bins}	d	Δt	v_r	α	δ	$\bar{m}_{N0}$	b_{N0}
200 km	1700 km	50	30 km	5 years	10 km/s	0.2	10	0.64 kg	0.18 m

Figure 5 (a) shows the collision probability between species where the debris populations M and N are characterized by the mass allocation parameter $\varepsilon = 0.5$. In this case, the mass of N is double that of M. Note the symmetry between species where $\phi_{i,j} = \phi_{j,i}$ and $n_{i,j} = n_{j,i}$. Since ϕ only depends on the size parameter of the object, there is no differentiation between S and D; however, there is a difference shown in the number of fragments in a collision between species is shown in Figure 5 (b). Collision between the debris M and N with any other object is considered to be non-catastrophic due to the low energy of impact. Only the mass of the lighter object is considered for the number of debris produced for a non-catastrophic collision [30], which results in this distribution.

4.2 Expanded payload and derelict populations for a 5-species model

As the payload and derelict satellite classes are inherently related expanding the payload species will require expanding the derelict species. The additional payload and derelict population results in a 5-species model, which is described in this section. The interaction of species per shell is visualized in Fig. 6. Note that there are now two payload classes (S_+

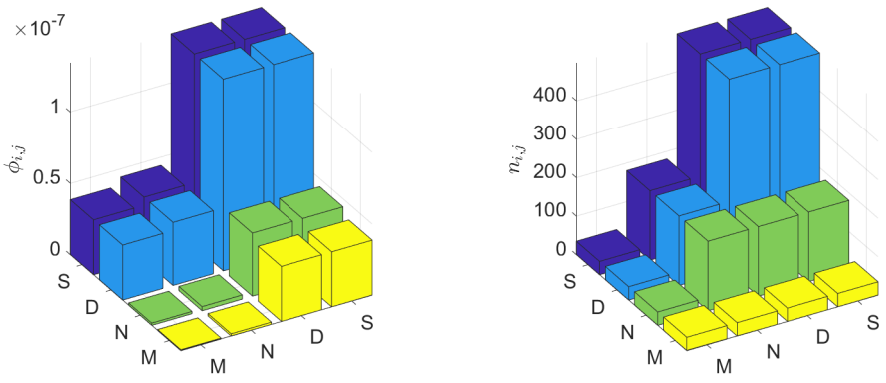

(a) $\phi_{i,j}$ (b) $n_{i,j}$

Fig. 5: Annualized collision probability between species ($\phi_{i,j}$) and number of fragments created per collision between species ($n_{i,j}$) for the 200 km shell and mass distribution of $\varepsilon = 0.8$

for the large payloads and S_- for small payloads) as well as derelict classes (D_+ and D_- for large and small derelict objects respectively). The population interaction coefficients ($\dot{\mathbf{C}}$) are described in Table 3. Note that this sampling over size or mass of the species can be extended into any number of bins, and schema is shown for expansion into two classes per species.

Table 3: Pairwise interactions between the species for the expanded payload model (5-species model)

	Species	**S_+ (Large satellites)**	**S_- (Small satellites)**	**D_+ (Large derelict)**	**D_- (Small derelict)**	**N (Debris)**
$\dot{C}$ Collision Source	**S_+**	$-\alpha_a\phi_{11}S_+^2$	$-\alpha_a\phi_{12}S_+$	$\delta S(\phi_{12}D_+ +\phi_{13}N +\phi_{14}N)$	$\delta S_+(\phi_{12}D_+ +\phi_{13}N +\phi_{14}N)$	$n_{11}\phi_{11}\alpha_a S_+^2 +n_{12}\phi_{12}\alpha S_+D +n_{11}\phi_{11}\alpha S_+N +n_{12}\phi_{14}\alpha S_+N$
	S_-	$-\alpha_a\phi_{11}S_+S_-$	$-\alpha_a\phi_{11}S_-^2$	$\delta S_-(\phi_{12}D_+ +\phi_{13}N +\phi_{14}N)$	$\delta S_+(\phi_{12}D_- +\phi_{13}N +\phi_{14}N)$	$n_{11}\phi_{11}\alpha_a S_-^2 +n_{12}\phi_{12}\alpha S_-D +n_{11}\phi_{11}\alpha S_-N +n_{12}\phi_{14}\alpha S_-N$
	D_+	$-\phi_{12}(\delta+\alpha)S_+D_+$	$-\phi_{12}(\delta+\alpha)S_-D_+$	$-\phi_{22}D_+^2$	$-\phi_{22}D_+D_-$	$n_{22}\phi_{22}D_+^2 +n_{23}\phi_{24}D_+N$
	D_-	$-\phi_{13}(\delta+\alpha)S_+N$	$-\phi_{13}(\delta+\alpha)S_-N$	$-\phi_{23}ND_+$	$-\phi_{23}D_-^2$	$n_{34}\phi_{34}D_-N$
	N	$-\phi_{13}(\delta+\alpha)S_+N$	$-\phi_{13}(\delta+\alpha)S_-N$	$-\phi_{24}ND_+$	$-\phi_{24}ND_-$	$n_{34}\phi_{34}N^2$
m Mass [kg]	-	$(1-\varepsilon)\bar{m}_{S0}$	$(1+\varepsilon)\bar{m}_{S0}$	$(1+\varepsilon)\bar{m}_{D0}$	$(1-\varepsilon)\bar{m}_{D0}$	0.64
b Diameter [m]	-	$(1+\varepsilon)^{1/3}\bar{b}_{S0}$	$(1+\varepsilon)^{1/3}\bar{b}_{S0}$	$(1-\varepsilon)^{1/3}\bar{b}_{D0}$	$(1-\varepsilon)^{1/3}\bar{b}_{D0}$	0.18
A Area [m^2]	-	$(1+\varepsilon)^{2/3}A_{S0}$	$(1+\varepsilon)^{2/3}A_{S0}$	$(1+\varepsilon)^{2/3}A_{D0}$	$(1-\varepsilon)^{2/3}A_{D0}$	0.25

4.3 Initial debris population

Using MASTER 8.0.3, the following profile of debris is initialized into the simulated LEO environment spanning 200 to 2000 km [31]. The dataset for 1-1-2020 is used as the initial debris population for all simulations in this work. The initial distribution the debris mass, diameter and number per altitude is visualized in Fig. 7.

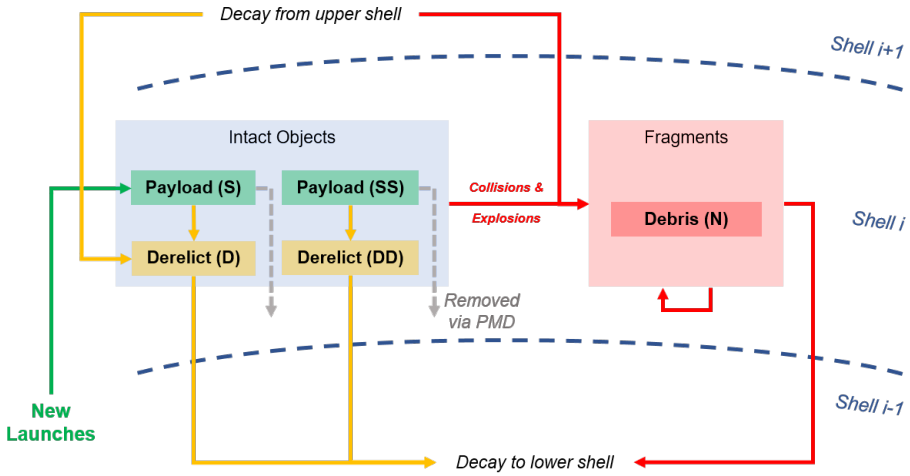

Fig. 6: Schematic for the 5-population model that includes an expanded debris population.

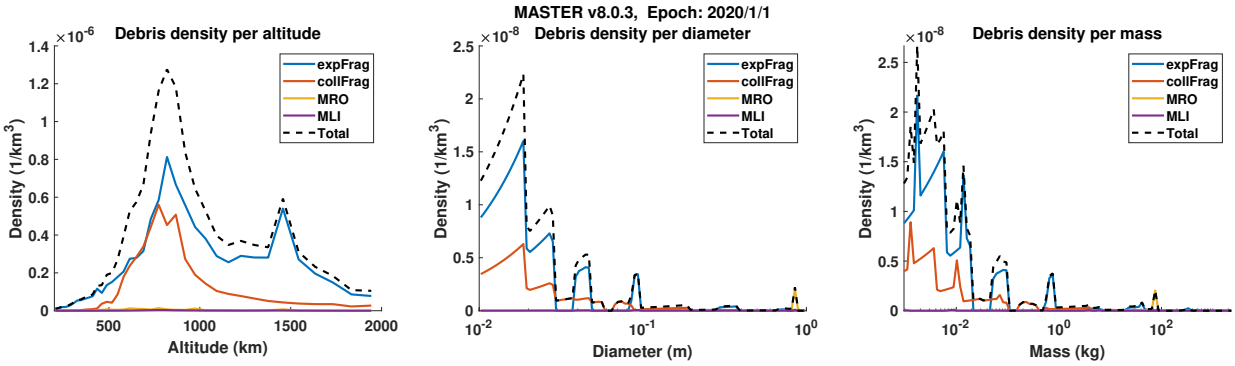

Fig. 7: Initial debris population from MASTER v8.0.3

5. RESULTS AND DISCUSSION

The LEO environment is initialized with the debris conditions taken from MASTER v8.0.3 for the year 2020. The debris population is visualized in Fig. 7 and described further in Section 4.3. A number of physical parameters are used as input to MOCAT, and a parameter sweep of $\varepsilon \in [0,1)$ is done on the mass of the objects, first on the debris class in Section **??** to result in a 4-species model. Any of the parameters can be expanded for any object type (A, C_D, α, etc), but the example shown here will focus on ε_{mass}.

The 3-species model with payload (S), derelict (D), and debris (N) species is expanded such that the debris species is further divided into small and large debris populations (N and M respectively) for a 4-species model. The only difference between the N and the M class property is in their mass as described in Table 1. For $\varepsilon = 0$ this 4-species model behaves identically as the 3-species model when the two debris populations are summed.

The propagation of the model using the initial conditions for the August 2022 TLE catalog with MASTER 8 debris population for objects greater than 5 cm and the launch rate of ITU filings (excluding the Rwanda constellation) replenish rate is shown in Fig. 9. ε ranges from 0.2 to 0.8, mainly showing the differences in the number of debris as propagated to 2200.

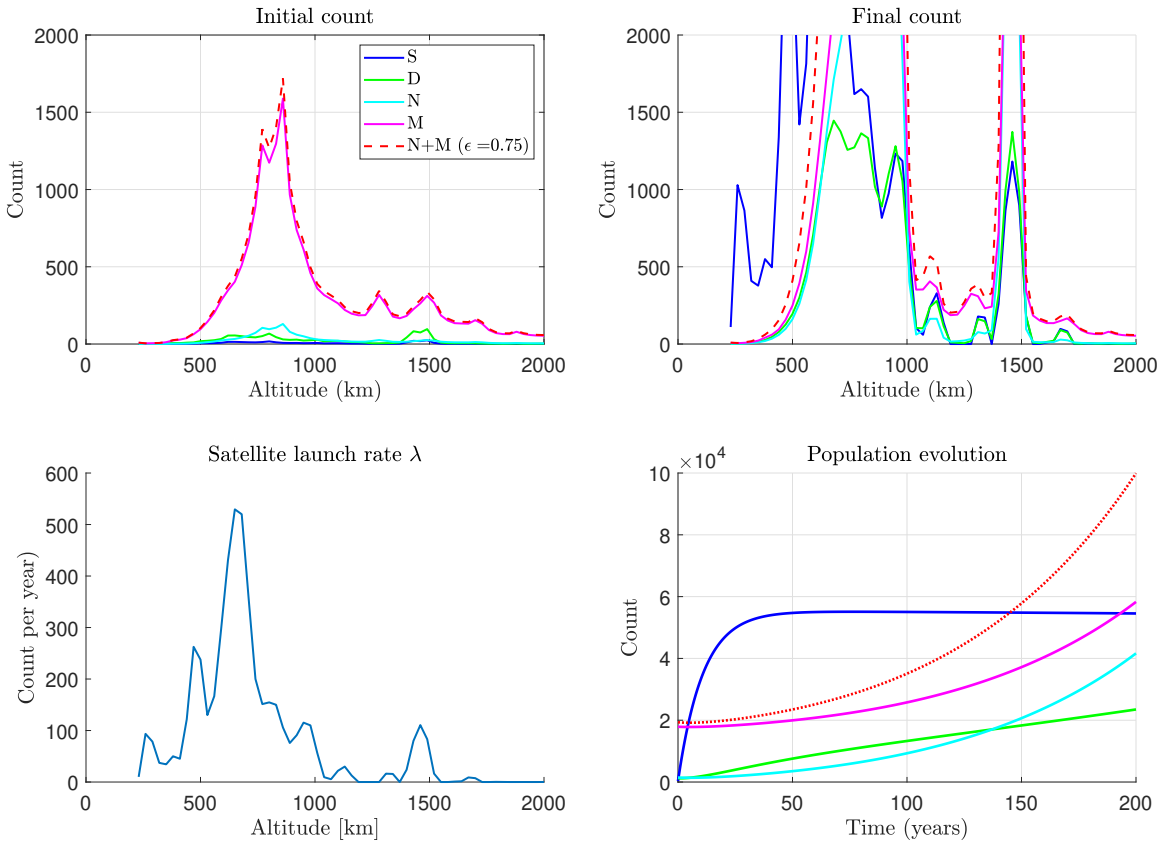

Fig. 8: Results for replacement-level launch rate (10x ITU) using $\varepsilon = 0.75$ for the expanded debris model

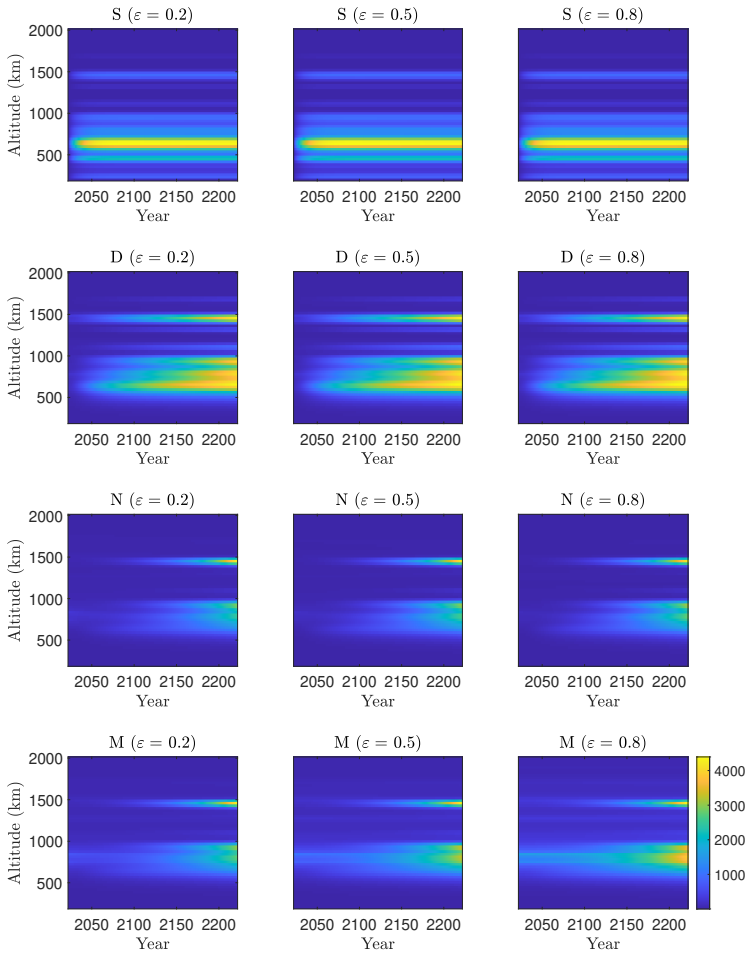

Fig. 9: Population evolution of the expanded debris model (4-species) for 200 years with mass distribution of $\varepsilon = 0.2$

6. CONCLUSION

This paper analyzed a method to discretize the physical parameters of chosen species. A 4-species model for two different categories of debris and a 5-species model for a two payload populations and two associated derelict populations are presented to sample a larger physical parameter space. Rather than a single averaged value across an entire population, variation to the physical properties can be extended through this method to any number of sampling points while — if need be — keeping the same overall population average values consistent with the generalized version. In essence, computational load of creating more species is traded for higher fidelity of sampling the ASO population. We show a MOCAT formulation for a 5-species for the first time, allowing for higher fidelity model of the LEO ASOs, which shows dynamics that we expect. The results from the expanded species analysis in this paper show that a sufficient number of traits for an ASO species should be sampled in order to capture the full dynamics of the population. Non-linear dynamics of these traits — even within a population with otherwise identical interaction with other species and the environment — will exhibit divergent behaviors compared to the simplified mean-only models of the population. Future works will further investigate the extent to which a number of sampling is sufficient to capture the dynamics, and which parameters would be worthwhile expanding the species. Validation of the model performance will be done using comparisons to other SSEM models as well as Monte-Carlo-based simulations of the LEO populations.

ACKNOWLEDGEMENTS

This work is sponsored by the Defense Advanced Research Projects Agency (Grant N66001-20-1-4028), and the content of the information does not necessarily reflect the position or the policy of the Government. No official endorsement should be inferred. Distribution statement A. Approved for public release. Distribution is unlimited.

7. REFERENCES

[1] ITU e-Submission of Satellite Network Filings - CINNAMON-937 9 2021.
[2] ITU e-Submission of Satellite Network Filings - AETHER-C 12 2021.
[3] D. J. Kessler and B. G. Cour-Palais, Collision Frequency of Artificial Satellites: The Creation of a Debris Belt *J Geophys Res*, vol. 83, pp. 2637–2646, 1978.
[4] H. G. Lewis, G. G. Swinerd, R. J. Newland, and A. Saunders, The fast debris evolution model *Advances in Space Research*, vol. 44, pp. 568–578, 9 2009.
[5] The Impacts of Large Constellations of Satellites *JASON report*, 2020.
[6] A. Rossi, G. B. Valsecchi, and E. M. Alessi, The Criticality of Spacecraft Index *Advances in Space Research*, vol. 56, pp. 449–460, 8 2015.
[7] H. Krag, S. Lemmens, and F. Letizia, Space traffic management through the control of the space environment's capacity *5th European Workshop on Space Debris Modeling and Remediation*, 2018.
[8] D. McKnight, R. Witner, F. Letizia, S. Lemmens, L. Anselmo, C. Pardini, A. Rossi, C. Kunstadter, S. Kawamoto, V. Aslanov, J. C. D. Perez, V. Ruch, H. Lewis, M. Nicolls, L. Jing, S. Dan, W. Dongfang, A. Baranov, and D. Grishko, Identifying the 50 statistically-most-concerning derelict objects in LEO *Acta Astronautica*, vol. 181, pp. 282–291, 4 2021.
[9] J. C. Liou, D. T. Hall, P. H. Krisko, and J. N. Opiela, LEGEND – a Three-dimensional LEO-to-GEO Debris Evolutionary Model *Advances in Space Research*, vol. 34, pp. 981–986, 1 2004.
[10] H. Lewis, G. Swinerd, N. Williams, and G. Gittins, DAMAGE: a Dedicated GEO Debris Model Framework *3rd European Conference on Space Debris*, pp. 373–378, 3 2001.
[11] H. G. Lewis, A. Saunders, G. Swinerd, and R. J. Newland, Effect of thermospheric contraction on remediation of the near-Earth space debris environment *Journal of Geophysical Research: Space Physics*, vol. 116, 2011.
[12] J. Dolado-perez, R. D. Costanzo, and B. Revelin, Introducing MEDEE - a New Orbital Debris Evolutionary Model *Proc. 6th European Conference on Space Debris*, pp. 22–25, 4 2013.
[13] C. E. Martin, J. E. Cheese, and H. Klinkrad, Space Debris Environment Analysis with DELTA 2.0 *55th International Astronautical Congress*, 2004.
[14] J. Radtke, S. Mueller, V. Schaus, and E. Stoll, LUCA2 - An Enhanced Long-term Utility for Collision Analysis *Proc. 7th European Conference on Space Debris*, 2017.

[15] M. E. Sorge and D. L. Mains, IMPACT Fragmentation Model Improvements *AIAA/AAS Astrodynamics Specialist Conference*, 8 2014.
[16] X. W. Wang and J. Liu, An Introduction to a New Space Debris Evolution Model: SOLEM *Advances in Astronomy*, vol. 2019, 2019.
[17] J. Drmola and T. Hubik, Kessler Syndrome: System Dynamics Model *Space Policy*, vol. 44-45, pp. 29–39, 8 2018.
[18] A. J. Rosengren, D. K. Skoulidou, K. Tsiganis, and G. Voyatzis, Dynamical cartography of Earth satellite orbits *Advances in Space Research*, vol. 63, pp. 443–460, 1 2019.
[19] J.-C. Liou, A. Anilkumar, B. B. Virgili, T. Hanada, H. Krag, H. Lewis, M. Raj, M. Rao, A. Rossi, and R. Sharma, Stability of the Future LEO Environment - an IADC Comparison Study *Proc. 6th European Conference on Space Debris*, 2013.
[20] A. D'Ambrosio, M. Lifson, and R. Linares, The Capacity of Low Earth Orbit Computed using Source-sink Modeling *arXiv*, 2022.
[21] A. D'Ambrosio, S. Servadio, P. M. Siew, D. Jang, M. Lifson, and R. Linares, Analysis Of The Leo Orbital Capacity Via Probabilistic Evolutionary Model *AAS/AIAA Astrodynamics Specialist Conference*, 8 2022.
[22] M. Lifson, A. D'Ambrosio, D. Arnas, and R. Linares, How Many Satellites Can We Fit In Low Earth Orbit?: Capacity Integrating Risk-based And Intrinsic Methods 2022.
[23] A. D'Ambrosio, M. Lifson, D. Jang, C. Pasiecznik, and R. Linares, Projected Orbital Demand and LEO Environmental Capacity *Advanced Maui Optical and Space Surveillance Technologies (AMOS) Conference*, 2022.
[24] D. Jang and R. Linares, System-Level Risk Assessment of the Low Earth Orbit Environment *8th Annual Space Traffic Management Conference*, 3 2022.
[25] C. Pasiecznik, A. D'ambrosio, D. Jang, and R. Linares, A Dynamical Systems Analysis of the Effects of the Launch Rate Distribution on the Stability of a Source-Sink Orbital Debris Model *International Astronautical Congress*, 2022.
[26] G. L. Somma, Adaptive Remediation of the Space Debris Environment Using Feedback Control 7 2019.
[27] B. R. Bowman, True Satellite Ballistic Coefficient Determination for HASDM *Astrodynamics Specialist Conference and Exhibit*, 8 2002.
[28] Models of the Earth's Upper Atmosphere (CIRA-2012) 7 2012.
[29] D. A. Vallado, *Fundamentals of Astrodynamics and Applications*. Microcosm Press, 5 ed., 7 2022.
[30] N. L. Johnson, P. H. Krisko, J. C. Liou, and P. D. Anz-Meador, NASA's New Breakup Model of EVOLVE 4.0 *Advances in Space Research*, vol. 28, pp. 1377–1384, 1 2001.
[31] A. Horstmann, S. Hesselbach, C. Wiedemann, S. Flegel, M. Oswald, and H. Krag, Enhancement of S/C Fragmentation and Environment Evolution Models *European Space Agency*, 8 2020.
[32] J. c Liou, D. J. Kessler, M. Matney, and G. Stansbery, A New Approach To Evaluate Collision Probabilities Among Asteroids, Comets, And Kuiper Belt Objects *Lunar and Planetary Science XXXIV*, 2003.
[33] J. C. Liou, Collision activities in the future orbital debris environment *Advances in Space Research*, vol. 38, pp. 2102–2106, 2006.